Room Temperature Ferroelectricity in $Na_{1-x}Sr_{x/2}\square_{x/2}NbO_3$ through the Introduction of Cationic Vacancies

A. Torres-Pardo,[†] R. Jiménez,[‡] J. M. González-Calbet,[†] and E. García-González*,[†]

Departamento de Química Inorgánica, Facultad de Químicas, Universidad Complutense, Madrid 28040, Spain, and Instituto de Ciencia de Materiales de Madrid, CSIC, Cantoblanco, Madrid 28049, Spain

Received July 31, 2008. Revised Manuscript Received September 30, 2008

The present study relates structural and microstructural modifications in the $Na_{1-x}Sr_{x/2}\square_{x/2}NbO_3$ solid solution with variations in the dielectric behavior when changing the chemical composition as an unprecedented investigation in lead-free ferroelectric compounds. X-ray diffraction, electron diffraction, and high resolution electron microscopy have been used as techniques to obtain a complete knowledge of the structural and microstructural evolution of the system as a result of the doping process. In this paper, we focus our attention in the relevant structural transition which occurs in the $0 < x \leq 0.2$ composition range correlated to the change in dielectric behavior observed from the electric characterization performed. The microstructural study performed in this system in correspondence with the exhaustive electric characterization provides evidence about the evolution suffered by the system in which the changeable A-vacancy concentration might play a crucial role by tuning the electric behavior.

Introduction

An important part of the investigations on lead-free environmentally friendly ferroelectric materials deals with perovskite-type solid solutions. In this way, ABO_3 perovskite-type compounds deriving from $BaTiO_3$ and $NaNbO_3$ have been chosen for this purpose. A lot of work has been devoted to study the influence on the phase transitions of ferroelectric perovskites of dopants substituting A and/or B ions. These substitutions can generate significant modifications in both the sequence and the character of the phase transitions which are important from a fundamental and a functional point of view. Most of the studies performed on $BaTiO_3$ and $NaNbO_3$ were focused on doped materials, since doping processes give rise to a significant improvement of the functional properties. $BaTiO_3$-derived materials have been prepared by homovalent substitutions as occurs in $Ba(Ti_{1-x}M_x)O_3$ and $Ba_{1-x}Ca_x(Ti_{1-x}M_x)O_3$[1] or heterovalent as in $Ba_{1-x}K_{x/2}La_{x/2}TiO_3$, $Ba_{1-x}A_{2x/3}\square_{x/3}TiO_3$ (A= La, Bi), $Ba_{1-x}\square_{x/2}(Ti_{1-x}M_x)O_3$, (M = Nb, Ta), $Ba_{1-x}A_x(Ti_{1-x}M_x)O_3$ (A = Na, K, M = Nb, Ta), $Ba(Ti_{1-x}Li_x)O_{3-3x}F_{3x}$, and $Ba_{1-x}K_x(Ti_{1-x}Mg_x)O_3$.[2−4] These materials exhibit electric properties corresponding to ferroelectric or relaxor ferroelectric materials depending on the chemical composition. The continuous change from ferroelectric to relaxor ferroelectric behavior is a characteristic feature of lead-free solid solutions while in lead containing perovskite type compounds only well defined compositions lead to relaxor character.[5] This gradual change has been investigated in $BaTiO_3$-based solid solutions,[6−8] but the low temperature of the ferroelectric-paraelectric phase transition in $BaTiO_3$ together with the poor piezoelectric properties make them suitable for applications based on their high value and nonlinearity of the dielectric constant.[9]

The relatively high temperature of the ferroelectric−paraelectric phase transition, the good ferroelectric properties, the need of lead free piezoelectric materials, and the discovery of relaxor ferroelectric behavior in sodium niobate based solid solutions[10,11] triggered the search for new compositions derived from $NaNbO_3$. Sodium niobate suffers a complex sequence of structural phase transitions.[12] The phase diagram of sodium niobate shows the antiferroelectric P phase as the stable polymorph at room temperature (T_c = 633 K) which can coexist with the ferroelectric Q phase for temperatures in the approximate range 393−533 K.[13,14] This ferroelectric phase can be induced by applying an electric field[15] or through the formation of adequate solid solutions, as is the case of $NaNbO_3-ABO_3$ (ABO_3 = $LiNbO_3$, $KNbO_3$)

* Corresponding author. Tel: +34-913944518. Fax: +34-913944352. E-mail: esterg@quim.ucm.es.
[†] Universidad Complutense.
[‡] CSIC.

(1) Ravez, J.; Simon, A. *Eur. J. Solid State Inorg. Chem.* **1997**, *34*, 1199.
(2) Ravez, J.; Simon, A. *Solid State Sci.* **2000**, *2*, 525.
(3) Ravez, J.; Simon, A. *J. Solid State Chem.* **2001**, *162*, 260.
(4) Khemakhem, H.; Simon, A.; Von Der Mühll, R.; Rave, J. *J. Phys.: Condens. Matter* **2000**, *12*, 5951.
(5) Simon, A.; Ravez, J.; Maglione, M. *J. Phys.: Condens. Matter* **2004**, *16*, 963.
(6) Yasuda, N.; Ohwa, H.; Asano, S. *Jpn. J. Appl. Phys., Part I* **1996**, *35*, 5099.
(7) Sciau, P.; Calvarin, G.; Ravez, J. *Solid State Commun.* **2000**, *113*, 77.
(8) Lei, C.; Bokov, A. A.; Ye, Z.-G. *J. Appl. Phys.* **2007**, *101*, 084105.
(9) O'Neill, D.; Catalan, G.; Porras, F.; Bowman, R. M.; Gregg, J. M. *J. Mater. Science: Mater. Electron.* **1998**, *9*, 199.
(10) Raevski, I. P.; Prosandeev, S. A. *J. Phys. Chem. Solids* **2002**, *63*, 1939.
(11) Raevski, I. P.; Reznitchenko, L. A.; Malitskaya, M. A.; Shilkina, L. A.; Lisitsina, S. O.; Raevskaya, S. I.; Kuznetsova, E. M. *Ferroelectrics* **2004**, *299*, 95.
(12) Megaw, H. D. *Ferroelectrics* **1974**, *7*, 87.
(13) Lefkowitz, I.; Lukaszewicz, K.; Megaw, H. D. *Acta Crystallogr.* **1966**, *20*, 670.
(14) Konieczny, K. *Mater. Sci. Eng.* **1999**, *860*, 124.
(15) Shuvaeva, V. A.; Antipin, M; Yu Lindeman, S. V.; Fesenko, O. E.; Smotrakov, V. G.; Struchkov, Y. T. *Ferroelectrics* **1993**, *141*, 307.

10.1021/cm802101r CCC: $40.75
Published on Web 10/31/2008

materials[16,17] interesting for the development of high temperature ferroelectric devices.

In addition to the isovalent doping process, chemical substitutions leading to controlled nonstoichiometric compounds have been performed. In this way, $Na_{1-x}NbO_{3-x/2}$ oxides[18] and $NaNbO_{3-x}$[19] have been prepared to analyze the influence of the partial reduction of Nb(V) on the variation of the maximum temperature permittivity. However, the creation of a certain amount of oxygen vacancies does not modify the antiferroelectric character of sodium niobate. Substoichiometric compounds in the A sublattice have been also obtained by partial substitution of sodium by rare earth and alkaline-earth ions.[10,20] In this sense, Raevskaya et al.[21] have reported relaxor ferroelectric character for certain compositions in the $NaNbO_3-Sr_{0.5}NbO_3$ system. Actually, the search for new compositions with relaxor type behavior has been the aim of most of the recent studies devoted to $NaNbO_3$-derived materials, rather than studying the influence on the gradual variation of the electric properties of a continuous doping process in a systematic way. In the $NaNbO_3-Sr_{0.5}NbO_3$ system an A-vacancy position is associated to every introduced strontium atom. This system was previously studied by Mori et al.[22] who established the formation of two solid solutions $Na_{1-x}Sr_{x/2}\square_{x/2}NbO_3$ in the $0 \le x \le 0.03$ and $0.14 \le x \le 0.5$ composition ranges and the coexistence of both in the intermediate range. This structural discontinuity was also observed in the electric properties, compounds in the first solid solution being antiferroelectric and ferroelectric in the second one. However, no specific role is assigned to the increasing amount of A-vacancies and their influence on the dielectric properties.

Controlling the chemical composition which induces the adequate structural changes is the clue for understanding and tuning the dielectric properties. Although several studies relate structural modifications with variations in the dielectric behavior when changing the chemical composition in lead-containing compounds, no precedent of such an investigation in lead-free ferroelectric materials has been reported. In this sense, we have prepared the $Na_{1-x}Sr_{x/2}\square_{x/2}NbO_3$ solid solution ($0 \le x \le 0.4$, $\square$ = A vacancy position). X-ray diffraction, electron diffraction, and high resolution electron microscopy have been used as techniques to obtain a complete knowledge of the structural and microstructural evolution of the system as a result of the doping process. In this paper, we focus our attention in the relevant structural transition which occurs in the $0 < x \le 0.2$ composition range correlated to the change in dielectric behavior observed from the electric characterization performed.

Experimental Section

Samples with nominal composition $Na_{1-x}Sr_{x/2}\square_{x/2}NbO_3$ ($x = 0$, 0.1, 0.2, 0.3, and 0.4) were prepared by the conventional ceramic technique. Corresponding stoichiometric amounts of $SrCO_3$ (99.9%, Merck), Na_2CO_3 (99.5%, Merck), and Nb_2O_5 (99.99%, Aldrich) were mixed in an agate mortar and heated in platinum crucibles at 1173 K for 12 h to decompose the different carbonates. The resulting powders were reground in an agate mortar, pelleted, and heated in air at 1423 and 1473 K for compositions $0 \le x \le 0.2$ and $0.3 \le x \le 0.4$, respectively. Samples were finally cooled to room temperature at a cooling rate of 1.5 K min^{-1}.

Magnetic measurements were performed in a Quantum Design XL-MPMS superconducting quantum interference device magnetometer to determine the presence of Nb(IV). At 5 K and 1 T only diamagnetic signal was observed for all the samples so measurements did not indicate the presence of Nb(IV) in the samples.

Room temperature powder X-ray diffraction (XRD) patterns for all samples were collected on a Panalytical X'PERT PRO ALPHA 1 diffractometer with a Ge(111) primary beam monochromator prealigned for Cu $K\alpha_1$ radiation and equipped with a X'Celerator fast detector. Effective step time of 800 s and a step size of 0.017 (deg/2θ) were used to record data for Rietveld analysis[23] at room temperature.

Samples for transmission electron microscopy were ultrasonically dispersed in *n*-butanol and transferred to carbon coated copper grids. Selected area electron diffraction (SAED) experiments were carried out on a PHILIPS CM20FEG SuperTwin electron microscope. High resolution electron microscopy (HREM) was performed on a JEOL JEM300FEG electron microscope. Crystal by crystal chemical composition was determined by EDS X-ray microanalysis carried out on both a PHILIPS CM20 FEG Super Twin electron microscope supplied with an EDAX analyzer DX4 (super ultrathin window (resolution $\approx$ 135 eV)) and a JEOL JEM300FEG microscope equipped with an ISIS 300 X-ray microanalysis system (Oxford Instruments) with a LINK "Pentafet" EDS detector. The average cationic composition of the samples was determined on a JEOL 8900 "Super Probe" electron probe microanalyzer with five wavelength-dispersive spectrometers (WDS) operating at 20 kV and 50 μA.

Dielectric properties were measured on a precision LCR meter HP 4284A impedance analyzer. Measurements were carried out as a function of temperature (80−750 K) at selected frequencies between 10^2-10^6 Hz on disk-shaped specimens of 13 mm diameter and 0.9 mm thickness sintered in air at 1373 K for 24 h (density >95%). Gold paste (Dupont QG 150) sintered at 1123 K was used as an electrode. The polarization electric field ($P-E$) hysteresis loops were obtained by means of a homemade system based on the virtual ground technique. High voltage sine waves of 0.1 Hz frequency were applied by the combination of a HP3325B synthesizer/function generator and a bipolar operational power supply/amplifier (TREK 10/40 A), while charge was measured with a home-built charge to voltage converter.

The total pyroelectric coefficient of the samples as a function of the temperature was measured using a modification of the "direct method" that takes into account the local temperature derivative.[24] This method allowed the determination of the total pyroelectric coefficient at each temperature minimizing the effects of the trapped charge release and the increase in sample conductivity on increasing the temperature. Prior to the pyroelectric measurements the samples

(16) Jiménez, R.; Sanjuán, M. L.; Jiménez, B. *J. Phys.: Condens. Matter* **2004**, *16*, 7493.
(17) Ivliev, M. P.; Raevskii, I. P.; Reznichenko, L. A.; Raevskaya, S. I.; Sakhnenko, V. P. *Phys. Solid State* **2003**, *45*, 1984.
(18) Zhelnova, O. A.; Raevski, I. P.; Reznichenko, L. A. *Ferroelectr. Lett.* **1990**, *11*, 57.
(19) Molak, A. *Solid State Commun.* **1987**, *62*, 413.
(20) Mishchuk, D. O.; V'yunov, O. I.; Ovchar, O. V.; Belous, A. G. *Inorg. Mater.* **2004**, *40*, 1324.
(21) Raevskaya, S. I.; Reznichenko, L. A.; Raevski, I. P.; Titov, V. V.; Titov, S. V.; Dellis, J.-L. *Ferroelectrics* **2006**, *340*, 107.
(22) Mori, D.; Colin, J.-P; Le Roux, G.; Pateau, L.; Toledano, J.-C. *Mater. Res. Bull.* **1973**, *8*, 1089.
(23) Rodríguez-Carvajal, J., Roisnel, T. *FullProf*, *WinPLOTR*, and accompanying programs at http:// www-llb.cea.fr/fullweb/powder.htmf, 1999.
(24) Jiménez, R.; Hungría, T.; Castro, A.; Jiménez-Riobóo, R. *J. Phys. D: Appl. Phys.* **2008**, *41*, 065408.

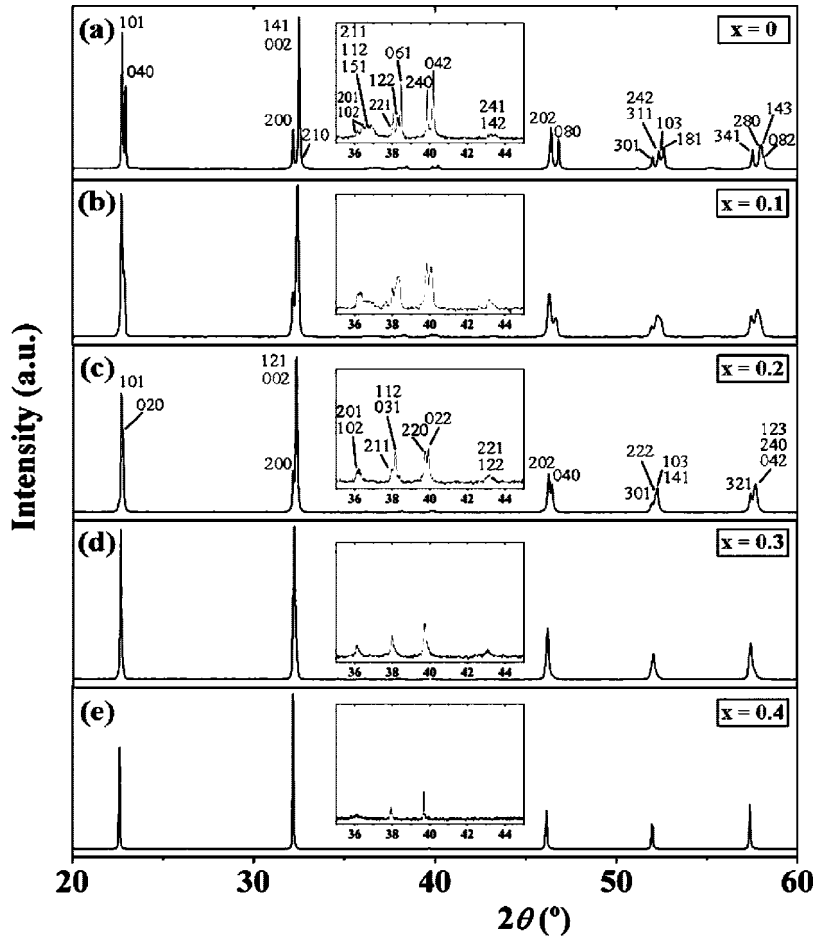

Figure 1. Room temperature powder XRD patterns corresponding to the (a) $x = 0$, (b) $x = 0.1$, (c) $x = 0.2$, (d) $x = 0.3$, and (e) $x = 0.4$ compositions of the $Na_{1-x}Sr_{x/2}\square_{x/2}NbO_3$ system. Miller indices are referred to the $\sqrt{2}a_c \times 4a_c \times \sqrt{2}a_c$ unit cell for $x = 0$ and $x = 0.1$ and to the $\sqrt{2}a_c \times 2a_c \times \sqrt{2}a_c$ unit cell for $x = 0.2$, 0.3, and 0.4 compositions.

were poled at 393 K applying a low frequency sinusoidal wave (0.01 Hz) with voltage amplitude large enough to produce saturation of the loop. After poling the sample is left in short-circuit condition for 24 h.

Results

The progressive substitution of strontium by sodium in the $Na_{1-x}Sr_{x/2}\square_{x/2}NbO_3$ system ($0 \le x \le 0.4$) retains the Nb(V) concentration at the expenses of the creation of a variable amount of A-cationic vacancies. Average cationic composition of all the samples was confirmed as the nominal composition by means of wavelength-dispersive spectroscopy. Crystal by crystal analysis performed by means of EDS X-ray microanalysis showed a Nb:Sr ratio always in agreement with the corresponding nominal composition. Sodium was present in all the crystals but its content was not quantified by this technique.

Structural and Microstructural Characterization. Figure 1 shows the room temperature powder XRD patterns corresponding to the $Na_{1-x}Sr_{x/2}\square_{x/2}NbO_3$ ($0 \le x \le 0.4$) solid solution. Single phase materials were obtained over the whole composition range. For strontium content above $x = 0.4$ a variable amount of a tetragonal tungsten bronze type-phase was always observed as the impurity phase. The XRD pattern of $NaNbO_3$ (Figure 1a) could be indexed, as expected, on the basis of the orthorhombic P phase,[25] space group *Pbma* (No. 57) with cell parameters $a \approx c \approx \sqrt{2}a_c$, $b \approx 4a_c$ (a_c refers to the unit cell parameter of the cubic perovskite sublattice).

The room temperature XRD patterns of strontium substituted samples show that the intensity of the reflections corresponding to the fourfold orthorhombic perovskite superstructure decreases when strontium content increases (see insets in Figure 1). In this sense, for the $x = 0.1$ composition very low intensity (211), (112), and (151) reflections indicate that the fourfold superstructure continues being present in this sample (called P-like phase in what follows) (inset in Figure 1a,b). The XRD pattern for the $x = 0.2$ composition (Figure 1c) could be assigned to a twofold orthorhombic perovskite superstructure, space group $P2_1ma$ (No. 26) with cell parameters $a \approx c \approx \sqrt{2}a_c$, $b \approx 2a_c$, isostructural to the Q-phase of the sodium niobate[15] (Q-like phase in what follows). In the case of $x = 0.3$ and 0.4 (Figures 1d,e, respectively), a significant decrease of the splitting of the diffraction maxima is observed. However, the presence of superstructure reflections in respect to the basic perovskite-type cell (around 36 and 38°/2θ) leads us

(25) Sakowsky-Cowley, A. C.; Lukaszeswicz, K.; Megaw, H. D. *Acta Crystallogr., Sect. B* **1969**, *25*, 851.

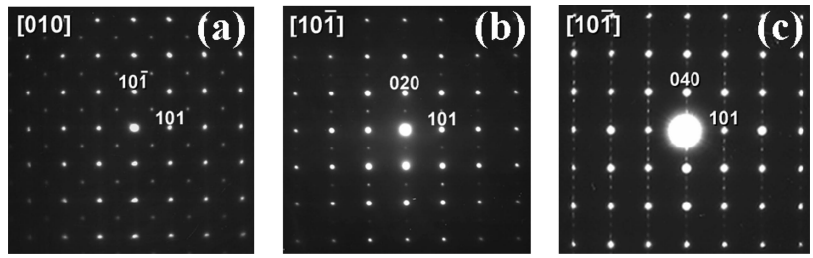

Figure 2. SAED patterns of $Na_{0.9}Sr_{0.05}NbO_3$ taken along the (a) [010], (b) [10$\bar{1}$] $DOMAIN_A$, and (c) [10$\bar{1}$] $DOMAIN_B$ zone axes. (A and B are the corresponding domains shown in Figure 3a). Miller indices refer to the $\sqrt{2}a_c \times 2a_c \times \sqrt{2}a_c$ unit cell (space group $P2_1ma$) for domain A and to the $\sqrt{2}a_c \times 4a_c \times \sqrt{2}a_c$ unit cell (space group *Pbma*) for domain B.

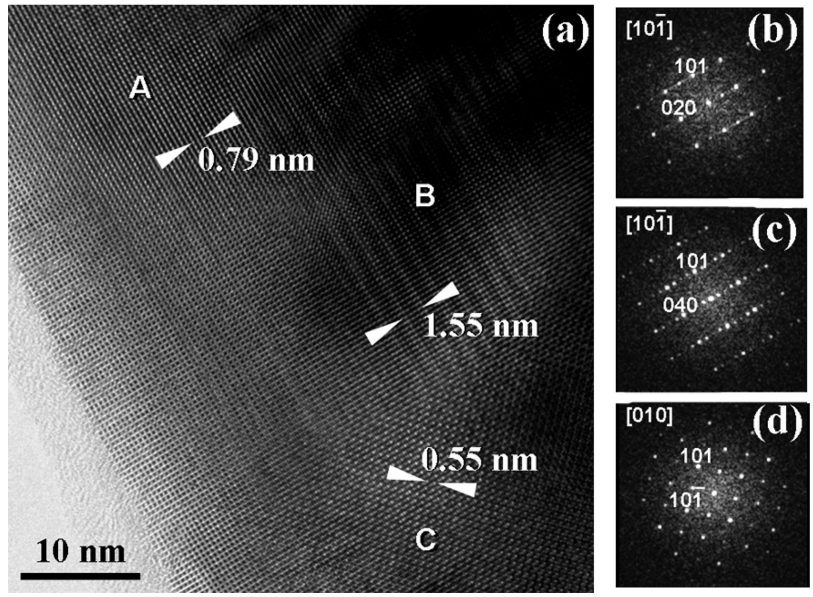

Figure 3. (a) High resolution electron micrograph of a crystal of $Na_{0.9}Sr_{0.05}NbO_3$ in the [010] projection. Areas of different periodicities (A, B, and C) are observed. Fourier transform corresponding to (b) area A, (c) area B, and (d) area C are shown.

to assign maxima on both diffraction patterns on the basis of an orthorhombically distorted $\sqrt{2}a_c \times 2a_c \times \sqrt{2}a_c$ perovskite-type cell although their relative intensity becomes very low in the case of the $x = 0.4$ composition.

Therefore, an important structural modification between the fourfold superstructure (P-like phase) observed for $x = 0.1$ to the twofold superstructure (Q-like phase) of the $x = 0.2$ composition occurs. This structural change might be associated with a change in the electrical properties from the antiferroelectric to ferroelectric behavior by analogy with $NaNbO_3$ when doped with other alkaline elements,[16,17] where the Q-like phase is obtained as a unique phase for a certain threshold value, thus giving rise to a homogeneous ferroelectric material. Since the doping process in $Na_{1-x}Sr_{x/2}\square_{x/2}NbO_3$ takes place through the introduction of important amounts of A-vacancies, it is not illogical to think that they must play a role in the electric response of the materials. Correlation between A-vacancies creation and ferroelectric behavior is not a well studied phenomenon, and no other examples on lead-free ferroelectric materials are known. In this sense, we have performed an exhaustive study of the microstructure and the electrical behavior in the $0 < x \leq 0.2$ composition range.

Figure 2a corresponds to the SAED pattern of the $Na_{0.9}Sr_{0.05}NbO_3$ sample taken along the [010] zone axis. Diffraction maxima show the orthorhombic distortion of the perovskite basic unit cell with parameters $a \approx c \approx \sqrt{2}a_c$. Notice that the forbidden (100) reflection is observed by multiple diffraction. In the [10$\bar{1}$] zone axis (Figure 2b), diffraction spots appear doubling the [010] reciprocal direction indicating that, for the $x = 0.1$ composition, crystals show a unit cell with parameters $\sqrt{2}a_c \times 2a_c \times \sqrt{2}a_c$ (Q-like phase). However, some SAED patterns display, in the same orientation, a fourfold superstructure along [010] reciprocal direction, indicating the formation of the $\sqrt{2}a_c \times 4a_c \times \sqrt{2}a_c$ (P-like phase) unit cell (Figure 2c). The HREM micrograph of a crystal of the $Na_{0.9}Sr_{0.05}NbO_3$ composition taken along the [10$\bar{1}$] zone axis is shown in Figure 3. Distances of 0.79 nm are apparent in the zone labeled as A indicating the doubling of the *b*-axis. In addition, areas with periodicity of 1.55 nm along [010] (area labeled B) show up the fourfold superstructure in respect to the cubic perovskite. Such features are confirmed by the corresponding Fourier transform, performed on each area (Figures 3b,c, respectively). A third type of structural domain can be observed (area labeled C) which is common to both the P- and the Q-like phases projected on the (010) plane with measured distances of 0.55 nm. From the transmission electron microscopy characterization, the domains of the P-like phase seem to appear in the crystals in a lower concentration than domains of the Q-like phase. These results are consistent with our previous observation from the analysis

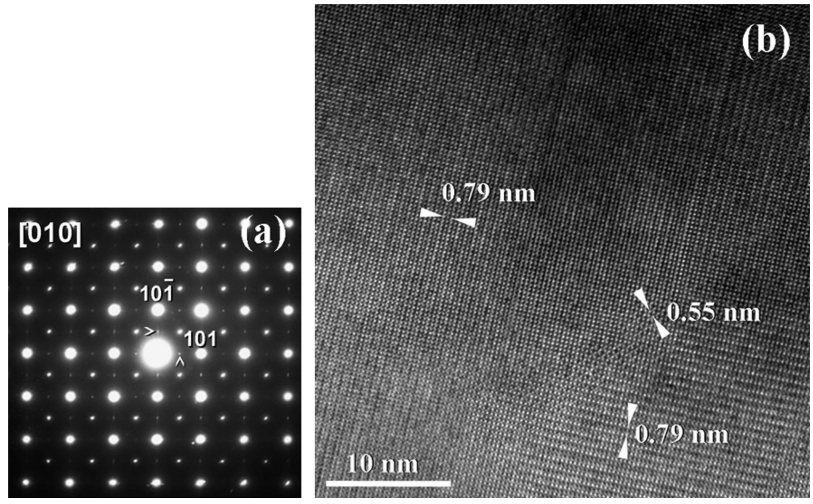

Figure 4. (a) SAED pattern of $Na_{0.8}Sr_{0.1}NbO_3$ taken along [010] zone axis. Arrows show diffraction maxima corresponding to the [10$\bar{1}$] reciprocal projection oriented in the two perpendicular directions. (b) Corresponding high resolution electron micrograph where areas with the three different perpendicular orientations are observed.

of the corresponding powder XRD data, where fourfold superstructure diffraction maxima displayed lower intensity than the undoped material. At this point, it is important to mention that no deviation from the nominal composition has been found neither in one structural domain type nor in the other one. The average estimated domain size is around 500 nm and no evidence of strontium/sodium/vacancy order is found so a random distribution of vacancies seems to occur in the A sublattice of the material. Therefore, crystals of $Na_{0.9}Sr_{0.05}NbO_3$ are constituted by structural domains of both, a P-like and a Q-like phase where the latter appears as major component at room temperature.

Figure 4a corresponds to the SAED pattern of a crystal of $Na_{0.8}Sr_{0.1}NbO_3$. The diffraction pattern can be interpreted as the overlapping of the corresponding diagrams taken along [010] and [10$\bar{1}$] reciprocal lattice projections of an orthorhombic $\sqrt{2}a_c \times 2a_c \times \sqrt{2}a_c$ unit cell (see Figure 2a,b for comparison), the last one being oriented in two perpendicular directions (recall that (100) reflection appears by multiple diffraction). SAED patterns showing the three separated orientations were not obtained, indicating a decrease of the average domain size. This interpretation is confirmed by the corresponding electron micrograph shown in Figure 4b. As observed, crystal is formed by structural domains of the Q-like phase oriented along the three perpendicular directions. The average estimated domain size is around 100 nm for this composition, the decreasing size being probably a consequence of the increase of the A vacancies concentration. Again, the electron microscopy study performed did not show any evidence of cation-vacancy order in the A sublattice of the perovskite-type structure. With this information, the structural refinement by Rietveld method was performed for $Na_{0.8}Sr_{0.1}NbO_3$ on the XRD data collected at room temperature. The experimental, calculated, and difference powder XRD profiles are shown in Figure 5. Fractional atomic coordinates belonging to the $P2_1ma$ space group (No. 26) were used as input data, by location of atoms in the atomic positions of a unit cell of periodicity $\sqrt{2}a_c \times 2a_c \times \sqrt{2}a_c$ similar to the unit cell previously described for the Q-phase

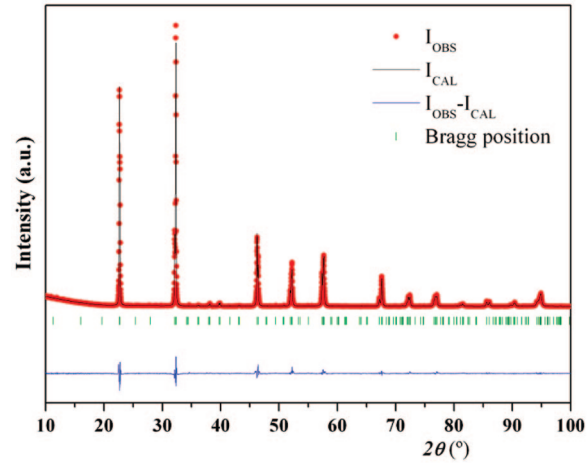

Figure 5. Rietveld refinement of the room temperature powder XRD pattern of $Na_{0.8}Sr_{0.1}NbO_3$. Experimental, calculated, and difference XRD profiles are shown.

Table 1. Crystallographic Data for $Na_{0.8}Sr_{0.1}NbO_3$ at Room Temperature

space group	$P2_1ma$ (No. 26)
a (nm)	0.567(2)
b (nm)	0.816(1)
c (nm)	0.530(6)
B_{iso} (Å^2)	0.532
R_p	7.98
R_{exp}	7.02
R_B	3.95
χ^2	2.80

of $NaNbO_3$.[15] Table 1 summarizes the crystallographic parameters of $Na_{0.8}Sr_{0.1}NbO_3$ at room temperature. The disordered distribution of strontium and sodium atoms in the 2*a* and 2*b* crystallographic sites of the structure as well as the random location of vacancies in the A sublattice of the perovskite-type structure are confirmed from the refined site occupancy factors (Supporting Information, Table S-1).

Dielectric Characterization. The gradual structural change observed at room temperature in the $0 \leq x \leq 0.2$ compositional range of the $Na_{1-x}Sr_{x/2}\square_{x/2}NbO_3$ system suggests that a progressive evolution of the electrical behavior takes place in these materials through the stabilization of the ferroelectric

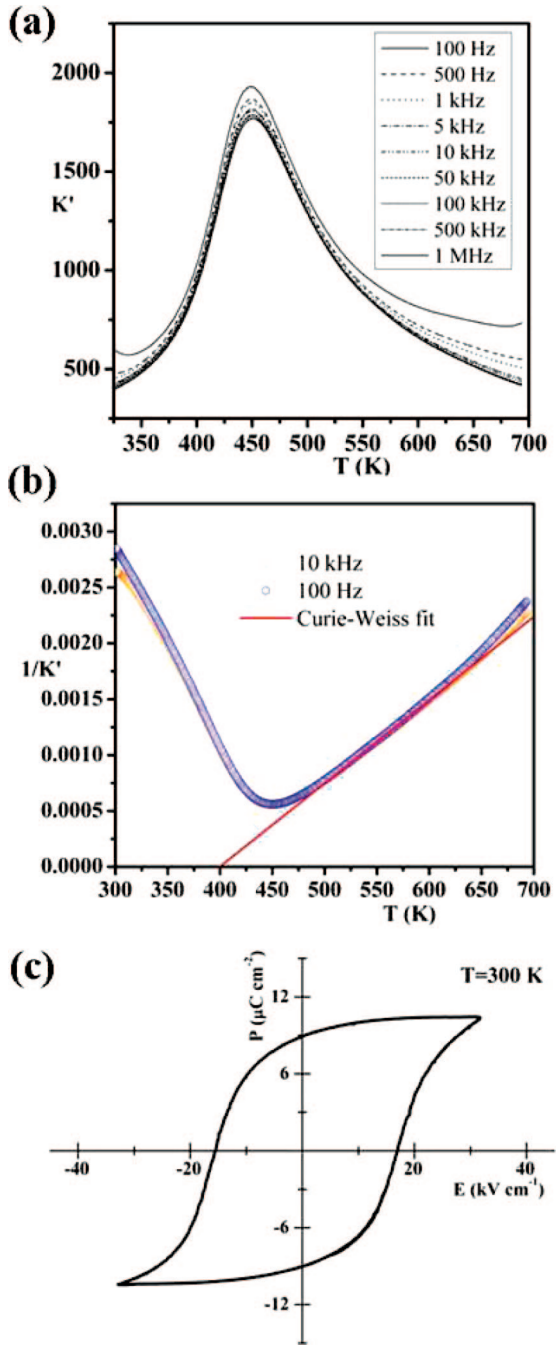

Figure 6. (a) Temperature dependence of K' at different measurement frequencies for $Na_{0.8}Sr_{0.1}NbO_3$. (b) Plot of $1/K'$ as a function of temperature measured at 100 Hz and 10 kHz showing the Curie−Weiss law fit. (c) Histeresis loop for the $Na_{0.8}Sr_{0.1}NbO_3$ material at 300 K. The $P(E)$ curve was measured at an applied field of 1.2 kV at the frequency of 0.1 Hz.

Q-like phase. In fact, Figure 6a shows the temperature dependence of the real part of the relative dielectric constant (K') for the $x = 0.2$ composition. A diffuse maximum of K' at $T_c = 448$ K without relaxation on frequency increasing is observed. From the shape of the maximum, the temperature dependence of K' obeys a Curie−Weiss law above T_c as shown by the linear $1/K'$ versus temperature response in Figure 6b. The Curie−Weiss constant value ($\sim 1.3 \times 10^5$ K) and the positive value (399 K) of the extrapolation of the linear fit to $1/K' = 0$ indicate a displacive ferroelectric-paraelectric phase transition. The diffuseness of the transition can be calculated fitting the experimental data to the equation proposed by Uchino and Nomura[26] for the paraelectric branch of the ferro-paraelectric transition: $1/K' = (1/K'_{max})\{1 + [(T - T_c)^{\gamma}/(2\delta^2)]\}$, where γ represents an empirical term that has a value of 1 for pure Curie−Weiss behavior and 2 for Gaussian shape that corresponds to a relaxor behavior and δ is the diffuseness parameter. The other parameters have their usual meaning. The large values obtained from the fitting of both $\gamma = 1.65 \pm 0.08$ and $\delta = 24 \pm 0.3$ indicate strong diffusivity of the phase transition that can related to the disorder between Sr and vacancy, the small domain size, and cell distortion. The material exhibits a typical ferroelectric hysteresis loop (P vs E) showing a remnant polarization (P_r) and a coercive field (E_c) with values of 9 μC cm^{-2} and 16 kV cm^{-1} at 300 K, respectively (Figure 6c). Therefore, $Na_{0.8}Sr_{0.1}NbO_3$ behaves as a ferroelectric material at room temperature.

The temperature dependence of K' at different measuring frequencies for the $x = 0.1$ composition is shown in Figure 7a. The obtained profile displays two maxima of K' at 543 and 563 K, without relaxation on frequency increasing. In addition, a wide small maximum in the 200−350 K range is also detectable when representing the dielectric loss (K'') as a function of the temperature at different measuring frequencies (Figure 7b). For comparison, the temperature dependence of K' and K'' for the pure sodium niobate is displayed in red color in Figure 7a,b, respectively. As observed in Figure 7a, the temperature of the most intense maximum, related to the P ↔ R phase transition in sodium niobate,[12,27] decreases 100 K in respect to the undoped material. The low temperature anomaly, associated to the Q phase stability range in $NaNbO_3$,[14,16,24] decreases around the same magnitude (see Figure 7b), therefore suggesting that the stability range of the Q-like phase is displaced toward room temperature for the $x = 0.1$ composition. This displacement of the stability range of the Q phase allowed us to pole the sample at room temperature to induce a ferroelectric phase in the whole volume that was not possible in the $NaNbO_3$ composition. Notice that the material shows low values for K'' which support the fact that there is no deviation from the nominal composition in the crystals.

From the polarization versus electric field ($P-E$) hysteresis loop, the P_r and the E_c were 13.3 μC cm^{-2} and 18 kV cm^{-1}, respectively, for the $Sr_{0.05}Na_{0.9}NbO_3$ sample at 423 K. When comparing these values with those of the $x = 0.2$ sample, both obtained at the same temperature from their respective T_c, it can be observed that the P value is higher for the $x = 0.1$ composition. This is consistent with the microstructural change described when increasing dopant content to $x = 0.2$.

To obtain information about the stability of the Q-like phase induced in the whole volume by poling, we have carried out the study of the temperature dependence of the polarization for the $Na_{0.9}Sr_{0.05}NbO_3$ sample using the modified "direct method".[24] The evolution of the thermal stimulated current (TSC) released by polarized samples on increasing the temperature has been used to reproduce the temperature dependence of the polarization in lithium

(26) Uchino, K.; Nomura, S. *Ferroelectr., Lett. Sect.* **1982**, *44*, 55.
(27) Bouziane, E.; Fontana, M. D.; Ayadi, M. *J. Phys: Condens. Matter* **2003**, *15*, 1387.

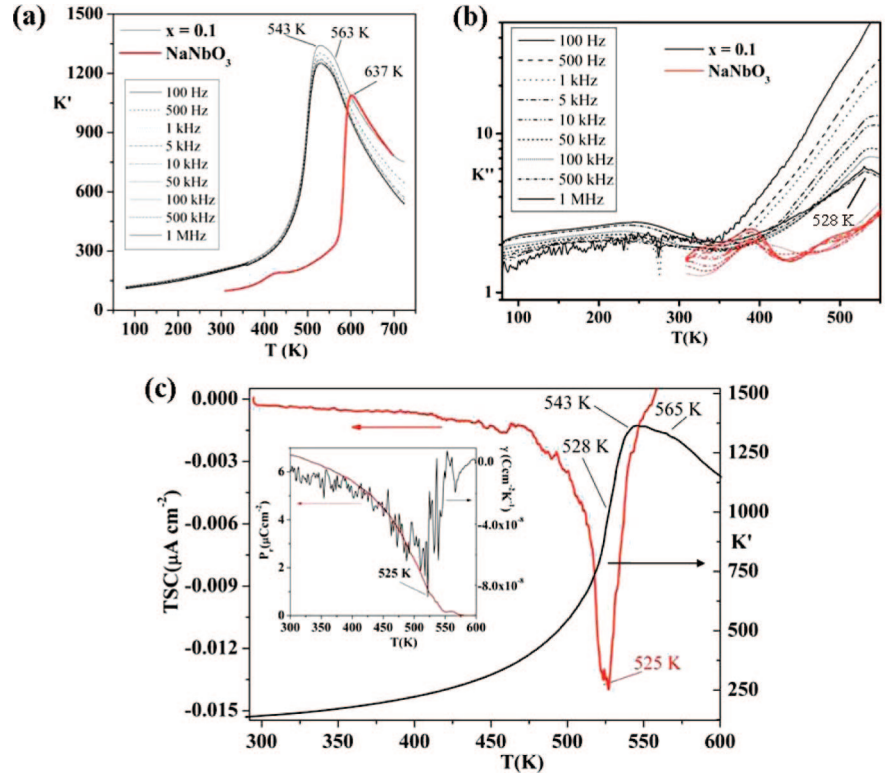

Figure 7. (a) Temperature dependence of K' at different measurement frequencies for $Na_{0.9}Sr_{0.05}NbO_3$. The temperature evolution of K' at 10 kHz for the pure sodium niobate is displayed as a red line. (b) Temperature dependence of K'' at different measurement frequencies for $Na_{0.9}Sr_{0.05}NbO_3$ (black lines) and $NaNbO_3$ (red lines). (c) TSC and relative dielectric constant measurement at 10 kHz corresponding to the $x = 0.1$ sample. The inset shows the temperature variation of both, the calculated pyroelectric coefficient and the polarization calculated from $\gamma(T)$.

substituted sodium niobate compounds. From this method, information about the temperature range in which the induced ferroelectric phase is stable has been obtained. Using the method, the total pyroelectric coefficient is calculated as a function of temperature from the thermo stimulated current (TSC). Then the polarization curve as a function of temperature is obtained for the polarized $Na_{0.9}Sr_{0.05}NbO_3$ sample. In Figure 7c the TSC released for the sample as a function of temperature is shown (red line) together with the evolution of the relative dielectric constant measured at 10 kHz (black line). The calculated pyroelectric coefficient as well as the evolution of the remnant polarization as a function of temperature are included in the inset. For this composition, the applied bias field at room temperature induces the ferroelectric phase in the volume of remaining antiferroelectric phase. The TSC and the calculated pyroelectric coefficient curves show a main peak at 525 K, far away from the temperature of the dielectric maximum (543 K). Since the polarized sample maintains most of its ferroelectric properties up to 525 K, a phase transition is expected for the material at this temperature which could be related with the reversion of the ferroelectric Q-like domains to another non ferroelectric phase at 525 K.[24,28] Effectively, a maximum in the evolution of K'' (Figure 7b) and a kink in the K' vs T curve (Figure 7c) are observed at 528 K, and this dielectric anomaly can be considered the signature of the Q to P reversion in this sample.

Discussion

The formation of the $Na_{1-x}Sr_{x/2}\square_{x/2}NbO_3$ solid solution implies the creation of an increasing amount of A vacancies when progressively increasing the strontium content. The microstructural study performed by transmission electron microscopy does not show any evidence of extra strontium/sodium/vacancy order in the perovskite A sublattice and, therefore, random distribution can be assumed. In the case of the $Na_{0.8}Sr_{0.1}NbO_3$ sample, which contains 10% of A vacancy positions, the Q-like phase is stabilized at room temperature in the form of structural domains oriented along the three perpendicular directions. The electrical characterization of this material shows the formation of a ferroelectric material with $T_c = 448$ K where the lack of frequency dispersion and other anomalies apart from the main ferroelectric−paraelectric phase transition supports considering this sample as a single ferroelectric phase.

The characterization performed on $Na_{0.9}Sr_{0.05}NbO_3$, which contains 5% of A vacancy positions, indicates that this material behaves as an intermediate state between the pure sodium niobate and the ferroelectric $Na_{0.8}Sr_{0.1}NbO_3$. Although its microstructure can be compared to that of $NaNbO_3$,[29] an increment of the relative amount of the ferroelectric Q-like phase domains is appreciated at room temperature. This qualitative observation is confirmed by the electrical behavior of the sample, since the temperature range of stability of the Q-like phase moves toward room temper-

(28) Wang, X. B.; Shen, Z. X.; Hu, Z. P.; Qin, L.; Tang, S. H.; Kuok, M. H. *J. Mol. Struct.* **1996**, *385*, 1.

(29) Chen, J.; Feng, D. *Phys. Status Solidi A* **1988**, *109*, 171.

ature (Figure 7b). Studies performed on sodium niobate and lithium substituted samples[13,24,28,30] have indicated that the stability of Q-phase domains is limited to a temperature range above which Q-phase domains revert to an antiferroelctric phase, similar to the P-phase. The TSC and the calculated pyroelectric coefficient curves obtained for $Na_{0.9}Sr_{0.05}NbO_3$ (Figure 7c) indicate that the Q-like phase domains appearing as a major component of crystals are stable up to 525 K. The loss of the polarization below the temperature of the main maxima in $K'(T)$ (543 K) suggests that the reversion to the P-like phase occurs at 525 K which, by analogy with $NaNbO_3$, turns into the antiferroelectric R and paraelectric S phases at 543 and 563 K, respectively.

Previous studies on this system[21] report a phase diagram in which the coexistence of the P and the Q-like phases is restricted to the $0.022 \leq x \leq 0.05$ composition range. When increasing strontium content between $x = 0.05$ to $x = 0.23$, the Q-like phase is stabilized although a ferroelectric material is only found above $x = 0.1$. The authors claimed that this is accompanied by an abrupt drop in the T_c values. Our structural characterization, however, has given a different view of the situation. Although a pure ferroelectric material is obtained for $x = 0.2$, transmission electron microscopy provides direct evidence of the intergrowth of P-type and Q-type phases at the domain scale for the $x = 0.1$ composition and only domains of Q-type phase for $x = 0.2$ are observed. X-ray diffraction patterns show the coexistence of the twofold and the fourfold superstructures for $x = 0.1$, but information about the microstructure of the materials can only be obtained through a direct observation of the crystals, which, in addition, might provide a valuable help in elucidating the role played by the A cationic vacancies in both the structure as well as the electric properties.

The substitution of 10% sodium by strontium in $Na_{1-x}Sr_{x/2}\square_{x/2}NbO_3$ generates analogue electrical properties than the introduction of 5% lithium[16] or 2% potassium[17,31] in $Na_{1-x}A_xNbO_3$ ($A = Li^+, K^+$). Both Li^+ and K^+ significantly differ from Na^+ in ionic radii,[32] the provoked structural distortion causing the loss of antiphase tilts around the orthorhombic *b* axis, responsible for the antiferroelectric fourfold superstructure. Ionic radii of Sr^{2+} and Na^+ are quite similar,[32] and thus, no significant distortion would be generated. However, every introduced strontium atom generates one A cationic vacancy, and it must be the pair [Sr-vacancy] that forces the loss of the fourfold superstructure in the $Na_{1-x}Sr_{x/2}\square_{x/2}NbO_3$ system. Therefore, the formation of the ferroelectric phase seems to need a critical [Sr-vacancy] concentration to be obtained as a unique phase. Transmission electron microscopy characterization performed has allowed having direct evidence that the ferroelectric phase stabilization takes place progressively as a result of the disappearance of the structural domains of the P-like phase at the expenses of the formation of domains of the Q-like phase. This gradual transformation occurs through the existence of an increasing amount of randomly distributed A vacancy positions which limits the growth of the structural domains diminishing their average size.

From the presented results, a question arises about the influence of further increase in the strontium content up to the limit of the solid solution formation. Doping the $Na_{0.8}Sr_{0.1}NbO_3$ ferroelectric material by increasing the A-vacancy content significantly changes the electrical properties of the materials to the observation of relaxor ferroelectric character. The microstructural study we have performed to complete the characterization of this system in correlation with the electric characterization provide evidence about the gradual evolution suffered by the system in which the changeable A-vacancy concentration might play a crucial role by tuning the electric behavior. A detailed study of the $Na_{1-x}Sr_{x/2}\square_{x/2}NbO_3$ solid solution in the $0.2 < x \leq 0.4$ composition range with a final overall discussion are presented as a separated work.

Acknowledgment. Financial support from DGICYT in Spain through Projects MAT2004-01248, MAT2007-61954, and MAT2007-61409 is gratefully acknowledged. Authors are grateful to Dr. J. Romero for the magnetic measurements and to the Centro de Difracción de Rayos X (U.C.M.) and to the Centro de Microscopía Electrónica Luis Bru (U.C.M.) for facilities.

Supporting Information Available: Crystallographic data in CIF format for $Na_{0.8}Sr_{0.1}NbO_3$ and summarizing Table S-1 showing final atomic positions and site occupancy factor at room temperature (PDF). This material is available free of charge via the Internet at http://pubs.acs.org.

CM802101R

(30) Reznichenko, L. A.; Shilkina, L. A.; Gagarina, E. S.; Raevskii, I. P.; Dul'kin, E. A.; Kuznetsova, E. M.; Akhnazarova, V. V. *Crystallogr. Rep.* **2003**, *48*, 448.
(31) Ahtee, M.; Glazer, A. M. *Acta Crystallogr.* **1976**, *A32*, 434.
(32) Shannon, R. D. *Acta Crystallogr.* **1976**, *A32*, 751.